Synergistic Effect between NO_2 and SO_2 in Their Adsorption and Reaction on γ-Alumina

Qingxin Ma, Yongchun Liu, and Hong He*

Research Center for Eco-Environmental Science, Chinese Academy of Sciences 18 Shuangqing Road, Haidian District, Beijing 100085, China

Received: March 7, 2008; Revised Manuscript Received: May 8, 2008

Field measurements showed that there exists a correlation between nitrate and sulfate on mineral dust. In this work, the synergistic mechanism of adsorption and reaction between SO_2 and NO_2 on gamma-alumina was studied using *in situ* diffusion reflectance infrared Fourier spectroscopy (*in situ* DRIFTS) and temperature programmed desorption (TPD). The results revealed that the reaction pathway of NO_2 adsorbed on alumina was altered in the presence of SO_2. In the absence of SO_2, nitrite was found to be an intermediate in the oxidation of NO_2 to surface nitrate species. However, in the presence of SO_2, the formation of nitrite was inhibited and a new intermediate, dinitrogen tetraoxide (N_2O_4), was observed. On the other hand, surface tetravalent sulfur species S(IV), including bisulfite and sulfite, were oxidized to sulfate in air condition when NO_2 was present. The atmospheric implication of this synergistic effect was also discussed.

Introduction

Sulfur dioxide (SO_2) and nitrogen oxides ($NOx = NO + NO_2$) are deleterious pollution gases in the atmosphere and their chemical activities are of great importance in atmospheric chemistry.[1] It is well-known that NOx plays a crucial role in the tropospheric photochemistry processes and atmospheric acid deposition. On the other hand, heterogeneous reactions of NOx on mineral dust also attract much attention because they not only alter the concentration of NOx but also change the surface properties of mineral dust which have important effects on the lifetime and cloud condensed nuclei (CCN) ability of dust aerosols.[2] There have been several laboratory studies of heterogeneous reactions of nitrogen oxides on the surface of a variety of atmospherically relevant particles, such as sea salt aerosols,[3–6] soot,[7–10] and mineral oxides.[11–15] The hydrolysis of NO_2 on particle surfaces was used to explain the discrepancy of HONO concentration between field observation and modeling predication.[10,13,14] The results of Barney[13] showed that NO_2 can be disproportioned to nitrous acid (HONO) and nitric acid (HNO_3) in the presence of adsorbed water. It means NO_2 can be viewed as either an oxidant or a reductant.

In the case of SO_2, it is well-known that SO_2 was the major precursor of sulfuric acid and sulfate aerosols. These aerosols are known to affect climate by scattering solar radiation, resulting in a net cooling effect (direct effect), as well as acting as cloud condensation nuclei (CCN), thus altering cloud properties and their associated impacts on radiation (indirect effect).[16] SO_2 can be oxidized to sulfate in aqueous aerosol and on sea salts by ozone and hydrogen peroxide.[17–19] The reactions of SO_2 on dust and mineral oxides were also reported.[20–22] However, the mechanism for SO_2 oxidation on mineral particles to form sulfate is uncertain yet. A number of models have been applied to predict the formation of sulfate aerosols on a global scale. The results showed that atmospheric SO_2 concentrations were typically overestimated by as much as a factor of 2, while sulfate tended to be underestimated,[23] implying that there are some unknown pathways for the formation of sulfate in the troposphere.

Mineral aerosol represents one of the largest mass fractions of the global aerosols. The annual flux of mineral aerosol to the atmosphere is estimated to be about 1000−3000 Tg.[24–26] Heterogeneous reactions of pollution gases which occur on the mineral aerosols surfaces play a critical role in the atmosphere chemistry.[27] Most laboratory studies of heterogeneous reactions on aerosol particles focus on NO_2 and SO_2, individually. However, little attention was paid to the synergistic effect between these pollutants in the adsorption and reaction processes on atmospheric aerosols. Recently, field measurements of the chemical composition of aerosol particles in East Asia showed an indication that particles originating from soil are more suitable for the internal mixture of sulfate and nitrate than other kinds of particles.[28] The observed correlation between sulfate and nitrate in these particles could be caused by surface reactions of sulfur and nitrogen species. Since SO_2 and NOx are always generated from the same sources, such as fossil and biomass combustion, and also coexist with relative high concentrations (in ppb level) in urban areas, it is reasonable to anticipate that there should be a synergistic effect between these pollutants. By now, only Ullerstam et al.[29] investigated the heterogeneous reactivity of SO_2 and NO_2 on Sahara Desert mineral dust with the main content being quartz and potassium feldspars. Their results showed that although there was no difference in uptake coefficients when SO_2 and NO_2 were introduced at the same time or introduced individually, NO_2 enhanced the formation of sulfate on dust surface. However, the interaction mechanism between SO_2 and NO_2 on mineral oxides is still needed to be further investigated.

Alumina is a major component of mineral dust in the atmosphere. In this study, γ-alumina was chosen as a model oxide of mineral aerosol to investigate the mechanism of the synergistic effect on the adsorption and reaction of SO_2 and NO_2 using *in situ* diffuse reflectance infrared fourier spectroscopy (*in situ* DRIFTS) and temperature programmed desorption (TPD). Although α-Al_2O_3 is the most common phase of alumina in the troposphere, γ-Al_2O_3 was also widely used as a model

* Corresponding author. Telephone: +86-10-62849123. Fax: +86-10-62923563. E-mail: honghe@rcees.ac.cn.

10.1021/jp802025z CCC: $40.75
Published on Web 06/26/2008

oxide for its better quality of spectra information to obtain useful information about the mechanism of atmospheric heterogeneous reaction. Many heterogeneous reactions on α- and γ-alumina show the similar catalytic mechanism. The results of this work should be useful for understanding the complex atmospheric chemistry about SO_2, NO*x*, and atmospheric particles in molecular level.

Experimental Section

In order to obtain high quality of spectral information of surface species, γ-Al_2O_3 with high specific surface area was used in experiments. The Al_2O_3 sample was prepared from boehmite (AlOOH, Shangdong Aluminum Corporation) by calcining at 873 K for 3 h. The sample was characterized by X-ray diffractometry using a computerized Rigaku D/mas-RB diffractometer (Japan, Cu Kα radiation, 1.54056 nm). The step scans were taken over a 2θ range of 10−90° in steps of 0.02°/s. The alumina sample was identified as γ-Al_2O_3 with the three main 2θ peaks at 67, 46, and 37°. The nitrogen adsorption−desorption isotherms were obtained at 77 K over the whole range of relative pressures, using a Micromeritics ASAP 2000 automatic equipment. Specific areas were computed from these isotherms by applying the Brunauer−Emmmett−Teller (BET) method. The BET area of the sample is 257 m^2/g. Before DRIFTS measurement, the γ-Al_2O_3 sample was pretreated in an *in situ* infrared cell by heating in 100 mL/min of synthesized air (20% O_2 + 80% N_2) at 573 K for 3 h. In order to simulate the actual polluted air, NO_2 for the experiments was synthesized from the reaction between NO (1.03% + N_2, Beijing Huayuan) and O_2 (99.999%, Beijing Huayuan). SO_2 (1.13% + N_2, Beijing Huayuan) and N_2 (99.999%, Beijing Huayuan) were used as received. Distilled H_2O was degassed by heating prior to use.

In situ DRIFTS spectra were recorded on a NEXUS 670 (Thermo Nicolet Instrument Corporation) FT-IR, equipped with an *in situ* diffuse reflection chamber and a high-sensitivity mercury cadmium telluride (MCT) detector cooled by liquid N_2. The γ-Al_2O_3 sample (about 11 mg) for the *in situ* DRIFTS studies was finely ground and placed into a ceramic crucible in the *in situ* chamber. The total flow rate was 100 mL/min in all flow systems, and the volume of the closed system was about 30 mL. The reference spectrum was measured after the pretreated sample was cooled to 303 K in a synthesized air stream. The infrared spectra were collected and analyzed using a data acquisition computer with OMNIC 6.0 software (Nicolet Corp.). All spectra reported here were recorded at a resolution of 4 cm^{-1} for 100 scans. The low frequency cutoff below 1200 cm^{-1} is due to strong lattice oxide absorptions.

TPD (temperature programmed desorption) experiments of the SO_2-saturated γ-Al_2O_3 in the absence and presence of NO_2 were performed with a temperature-programmed tube oven, equipped with a quadrupole mass spectrometer (QMS, Hiden HPR 20). Before the measurement of desorption, 80 mg of γ-Al_2O_3 was placed in a tubular reactor. The sample was pretreated at 573 K for 1 h at a flow of 50 mL/min synthesized air (O_2 20%). After cooled to room temperature (303 K), the sample was exposed to 200 ppm SO_2 in the absence or presence of NO (200 ppm) for 12 h. For the desorption process, the carrier gas was kept at a flow rate of 50 mL of Ar/min while the temperature was increased at a temperature ramp rate of 20 K/min, and the effluent composition can be monitored continuously by using a quadrupole mass spectrometer.

Results

Heterogeneous Reaction of NO_2 on γ-Al_2O_3. For comparison with other studies, an experiment of NO_2 (NO + O_2) adsorption on alumina was conducted. The alumina sample was exposed to NO (200 ppm) balanced with synthesized air in a total flow of 100 mL/min at 303 K. The *in situ* DRIFTS spectra as function of time are shown in Figure 1. Several bands at 1650−1200 cm^{-1} region became predominant with increasing exposure time. These bands can be assigned to oxide-coordinated and water-solvated nitrate species.[11,12,15] The bands at 1560 and 1535 cm^{-1} were assigned to the degenerate υ_3 mode of oxide-coordinated monodentate, which has been split into two bands due to a loss of symmetry upon adsorption. The bands at 1580 and 1620 cm^{-1} were ascribed to bidentate and bridging nitrate, respectively. Because the remnant water in the nitrogen stream can not be removed completely in the flow system at room temperature, adsorptions due to water-solvated surface nitrate at 1425, 1386 and 1310 cm^{-1} are also apparent.[11,15,30] A band at 1230 cm^{-1}, which was attributed to bidentate nitrite,[11,12] initially grew quickly, and then decreased with time. It is suggested that nitrite was the intermediate in the conversion of adsorbed NO_2 to nitrate.

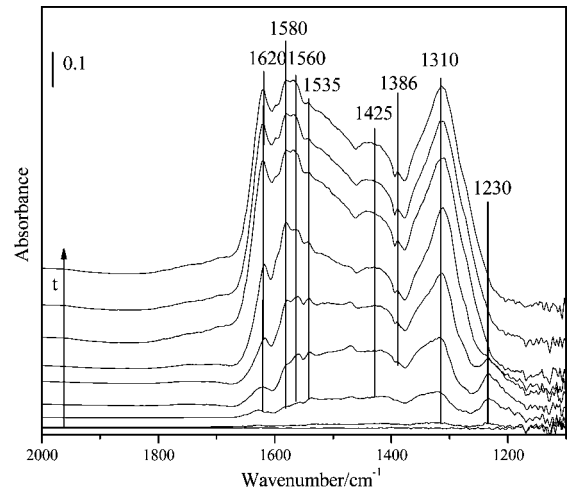

Figure 1. Dynamic changes in the *in situ* DRIFTS spectra of the γ-Al_2O_3 sample as a function of time (0, 1, 3, 5, 10, 15, 30, 45, 60 min) in a flow of 200 ppm NO + 20% O_2 + N_2 at 303 K.

The spectrum is very similar to the results reported by Miller et al.[15] where hydrated alumina was exposed to pure NO_2. Gas phase NO was not observed in the study because it was oxidized to NO_2 quickly in the presence of excess O_2. It is indicated that NO with excess O_2 can be used as a substitute of pure NO_2. Underwood et al.[11] postulated that nitrite species is an intermediate for the adsorption of NO_2 on oxides surface, and then form nitrate species and gas phase NO followed by a Langmuir−Hinshelwood (LH) type mechanism or a Eley−Rideal (ER) type mechanism. Our results are in agreement with this mechanism for the heterogeneous reaction of NO_2 on alumina.

Heterogeneous Reaction of SO_2 and NO_2 on γ-Al_2O_3. When SO_2 (200 ppm) was introduced simultaneously with NO (200 ppm) in the presence of excess oxygen (NO*x*), the *in situ* spectra were recorded as a function of time as shown in Figure 2. Nitrates were still the dominant surface species, which have been assigned to bridging[11] (1620 cm^{-1}), bidentate[11] (1580 cm^{-1}), monodentate[11] (1560 cm^{-1}), and water-solvated[15] (1417, 1310 cm^{-1}). It is worth to note that the peak at 1230 cm^{-1} assigned to nitrite[11,12] was clearly inhibited and two new peaks at 1733 and 1300 cm^{-1} rapidly increased in the early stages of the reaction, and then decreased in intensity as the reaction proceeded. These two peaks could be assigned to the asymmetric $\upsilon_a(NO_2)$ and symmetric $\upsilon_s(NO_2)$ stretch of the dimer of NO_2, namely, N_2O_4.[13,14,31,32] It indicates that the reaction pathway of

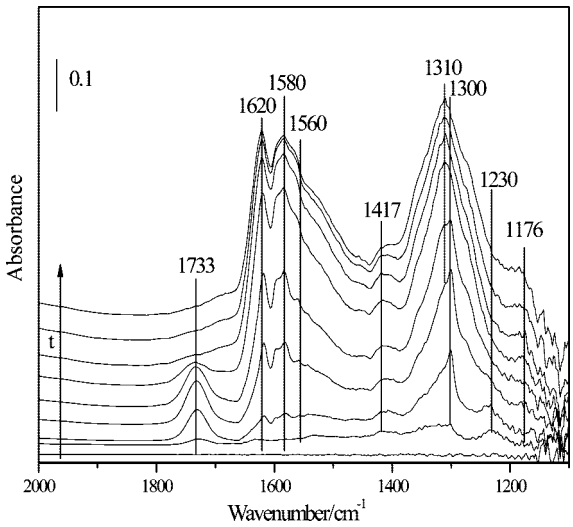

Figure 2. Dynamic changes in the *in situ* DRIFTS spectra of the γ-Al_2O_3 sample as a function of time (0, 3, 5, 10, 15, 30, 45, 60, 90 min) in a mixture flow of 200 ppm NO + 200 ppm SO_2 + 20% O_2 + N_2 at 303 K.

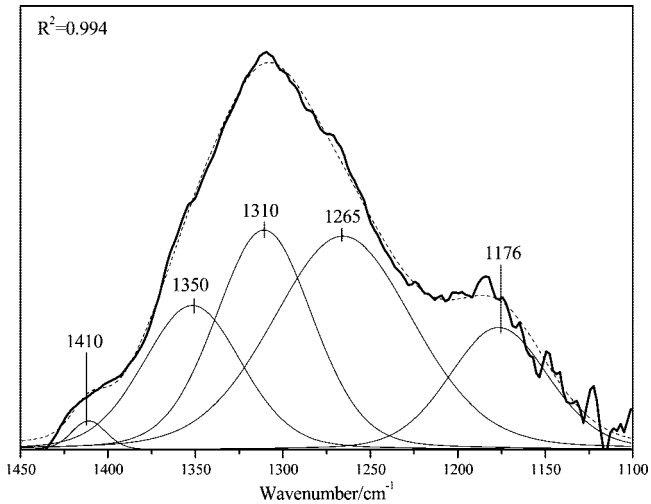

Figure 3. Peak fit of DRIFTS spectrum in the range of 1100−1450 cm^{-1} for the last spectrum in Figure 2.

NO_2 on γ-Al_2O_3 in the presence of SO_2 is different from that in the absence of SO_2. The mechanism will be discussed in the discussion section.

In addition, a peak at 1176 cm^{-1} could be assigned to the υ_s(OSO) vibration frequency of sulfate on alumina surface.[33,34] However, the peak near 1350 cm^{-1} for the υ_{as}(OSO) vibration frequency of sulfate on alumina surface[34] was not obviously observed which might be due to overlapping by the intense peak of solvated nitrate (1310 cm^{-1}). To further analyze the region from 1450 to 1100 cm^{-1}, a curve-fitting procedure using Lorenz and Gaussian curves based on the second-derivative spectrum was used to deconvolute overlapping bands,[12] as shown in Figure 3 with a correlation coefficient of 0.997. The bands at 1350 and 1176 cm^{-1} attributed to υ_{as}(OSO) and υ_s(OSO) vibration frequency of SO_4^{2-} were very clear. The appearance of a band at 1265 cm^{-1} was assigned to υ_3 mode of oxide-coordinated monodentate nitrate.[11] Obviously, when NO*x* and SO_2 present in the feed gases simultaneously, the reaction pathway of NO_2 on γ-Al_2O_3 surface was altered and SO_2 also could be oxidized to sulfate at room temperature.

Figure 4 shows the integrated absorbance of nitrate υ_3 of figure 1 and figure 2. Although the peak at 1620 cm^{-1} was also

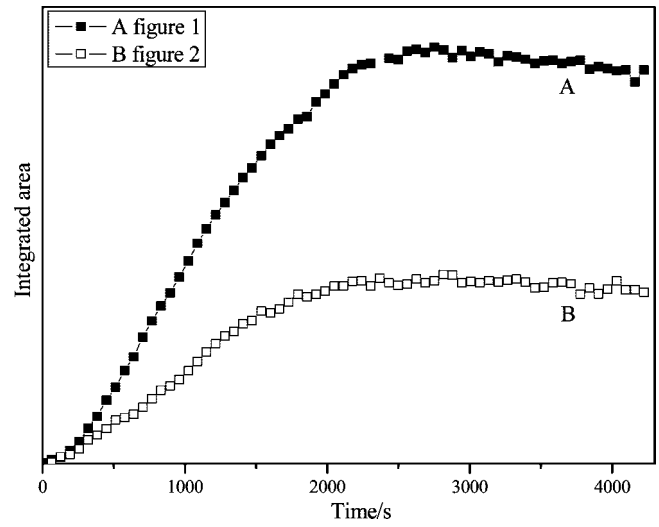

Figure 4. Integrated absorbance over the nitrate υ_3 band (1500−1600 cm^{-1}) observed during the reaction of NO_2 on alumina of Figure 1A and Figure 2B.

assigned to nitrate, the integrated range was chosen in 1600−1500 cm^{-1} to avoid the influence of surface water absorption. It is clear that nitrate species yielded from the adsorption of NO_2 on γ-Al_2O_3 in the absence of SO_2 (figure 4A) is faster than that in the presence of SO_2 (figure 4B). In the end, the sample got saturated and the total mount of nitrate decreased in the presence of SO_2 compared to the experiment without SO_2. A further analysis for reaction kinetic by DRIFTS is difficult because the evaluation of the diffusion depth and total sample area are unavailable in this study. However, the results supported that the reaction behavior of NO_2 adsorption on γ-Al_2O_3 was altered by the sulfur species.

Heterogeneous Reaction of SO_2 on γ-Al_2O_3. Since the presence of SO_2 could affect the adsorption of NO_2 on γ-Al_2O_3, it is necessary to investigate the reaction between SO_2 and γ-Al_2O_3. The alumina sample was exposed to 200 ppm SO_2 flow balanced with synthesized air at 303 K. As shown in Figure 5B, two peaks at 1630, and 1330 cm^{-1} are observed. The main feature of the spectra is a sharp band at 1630 cm^{-1} which could be assigned to the δ_{HOH} vibration of molecularly adsorbed water.[15,30,35,36] When the feed gases were dried with phosphorus pentoxide (P_2O_5) to remove the trace water in the feed gases, surface water at 1630 cm^{-1} still appeared in the spectra. It demonstrates that water was a product of the reaction between SO_2 and hydroxyl groups on γ-Al_2O_3 surface which will be discussed later. The band at 1330 cm^{-1} can be assigned to an asymmetric stretch (υ_3) of physisorbed SO_2.[21,22] When the sample was flushed with air, physisorbed SO_2 gradually disappeared. It is difficult to distinguish between surface sulfite and bisulfite species for the low signal-to-noise ratio and we generally named them surface tetravalent sulfur species S(IV).

As shown in Figure 5A, it should be noted that there is a drastic increase in the intensity of negative peaks at 3743 and 3704 cm^{-1}. In the model proposed by Peri,[37] these bands were attributed to the vibrations of surface hydroxyl (OH) species. The consumption of surface OH species means that the reaction between SO_2 and surface OH must occur.[36] The synchronous growth of a strong band at 1630 cm^{-1} and a broadband with a maximum at 3367 cm^{-1} in the spectra indicated that surface water was generated.

The reaction mechanism of SO_2 with alumina has been investigated widely. Karge et al.[38] studied the interaction of SO_2 with γ-Al_2O_3 using infrared spectroscopy. Using site blocking

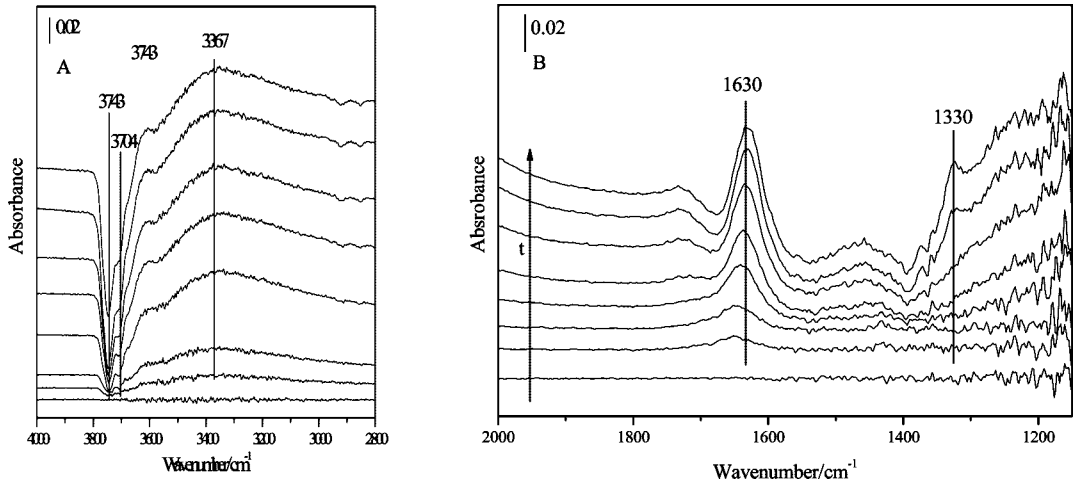

Figure 5. Dynamic changes in the in situ DRIFTS spectra of the γ-Al_2O_3 sample as a function of time (0, 3, 5, 10, 15, 30, 45, 60 min) in a mixture flow of 200 ppm SO_2 + 20% O_2 + N_2 at 303 K.

experiments with ammonia, pyridine and boron trifluoride, they determined that interaction of SO_2 with basic sites on the surface leads to formation of chemisorbed SO_2 while adsorption at acid sites leads to physisorbed SO_2. Datta et al.[39] further elaborated on the adsorption of SO_2 on γ-Al_2O_3. They reported that adsorption of SO_2 on Lewis acid (coordinately unsaturated alumina atoms) resulted in weakly adsorbed SO_2 and adsorption of SO_2 on Lewis base (exposed oxygen atoms) resulted in chemisorbed sulfite. Goodman et al.[21] studied the adsorption of SO_2 on α-Al_2O_3. They suggested SO_2 could react with lattice oxygen atom and surface OH to form surface sulfite and bisulfite. Surface water was also postulated as a product from the reaction between OH and SO_2.[21] No evidence was shown for the formation of sulfate in the mentioned studies. This work also supported their results. It is implied that SO_2 can hardly be oxidized to sulfate on alumina under air condition and at room temperature.

NO_2 Adsorption on a SO_2 Presaturated γ-Al_2O_3 Surface in a Closed Experiment. In order to further understand the redox process between NO_2 and surface tetravalent sulfur species S(IV), experiments in a closed system were performed at a low concentration. After exposed to a flow of SO_2 (50 ppm) balanced with synthesized air for 90 min, the alumina sample was exposed to a flow of NO (30 ppm) + O_2 (20%) for 15 min until the peaks at 1730 and 1300 cm^{-1} reached a maximal value, and then the inlet and the outlet valves were closed. The *in situ* DRIFTS spectra on the γ-Al_2O_3 sample were recorded as a function of time and are shown in Figure 6. It can be seen that the two peaks at 1730 and 1300 cm^{-1} disappeared synchronously, while the bands at 1410, 1351, 1230, and 1176 cm^{-1} increase in intensity. According to the above results, it can be deduced that the consumption of N_2O_4 led to the formation of surface sulfate (1351, 1176 cm^{-1}), water-solvated nitrate (1410 cm^{-1}), and nitrite (1230 cm^{-1}). The peak at 1624 cm^{-1} was due to water formed in the reaction of SO_2 with alumina surface. The shift from 1630 cm^{-1} (Figure 5) may be due to the combination with nitrate to form water-solvated nitrate. No oxide-coordinated (1530−1620 cm^{-1}) nitrate species were observed.

We can deduce that N_2O_4 can be readily accumulated on the SO_2 preadsorbed alumina surface because the active sites for the adsorbed NO_2 to form nitrite were occupied by S(IV) in the initial reaction stage. In addition, it should be noted that the peak intensity of surface water on alumina increased after the reaction with SO_2 since water was a product of the reaction

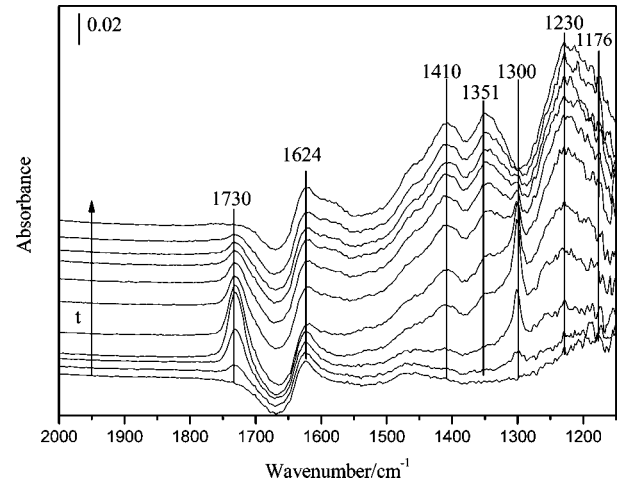

Figure 6. Dynamic changes in the *in situ* DRIFTS spectra of the SO_2 presaturated γ-Al_2O_3 sample as a function of time (0, 5, 10, 15, 20, 25, 30, 45, 60, 90, 120 min) in a closed atmosphere of 30 ppm NO + 20% O_2 + N_2 at 303 K.

between surface hydroxyl and SO_2. However, the effect of surface water on the formation of N_2O_4 is still unclear.

NO_2 Adsorption on H_2O_{ads}/γ-Al_2O_3. Since surface water was considered as a crucial factor for the enhancement of N_2O_4 on porous glass,[13,14] it is necessary to investigate the role of water in the heterogeneous reactions on γ-Al_2O_3 surface. Therefore, we looked into the adsorption of NO_2 on a water-saturated γ-Al_2O_3 surface at 303 K to investigate the role of water in this surface process. These experiments were conducted in a flow system. The alumina surface was exposed to a flow of water (RH = 2%) in synthesized air until saturation of water adsorption, and then the mixture gases of NO (200 ppm) + O_2 (20%) and water (RH = 2%) were introduced into the feed gases. All reactant gases were balanced with synthesized air. The *in situ* spectra of the alumina surface during this process are shown in Figure 7. The peak at 1650 cm^{-1} which was assigned to adsorbed water[15] disappeared after the sample was exposed to NO_2, accompanying with the appearance of bands due to surface nitrate species at 1620, 1580, 1560, 1425 and 1320 cm^{-1}. It indicates that the surface water was replaced by nitrate species or associated with nitrate to form water-solvated nitrate. However, the peaks at 1730 and 1300 cm^{-1} due to adsorbed N_2O_4 were not observed and a band at 1230 cm^{-1} which was attributed to nitrite[11,12] appeared in the initial

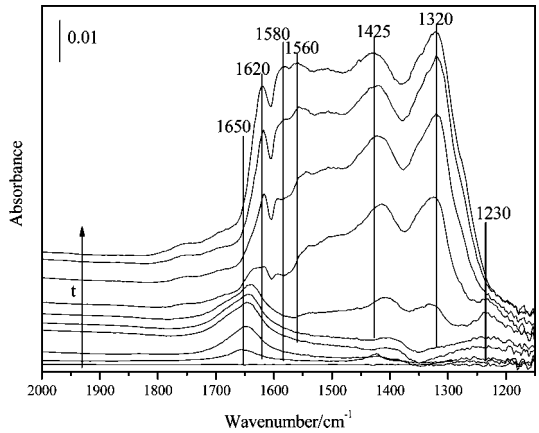

Figure 7. Dynamic changes in the *in situ* DRIFTS spectra of the H_2O presaturated γ-Al_2O_3 sample as a function of time (0, 3, 5, 10, 15, 20, 30, 45, 60, 90 min) in the flow of 200 ppm NO + 20% O_2 + N_2 (RH = 2%) at 303 K.

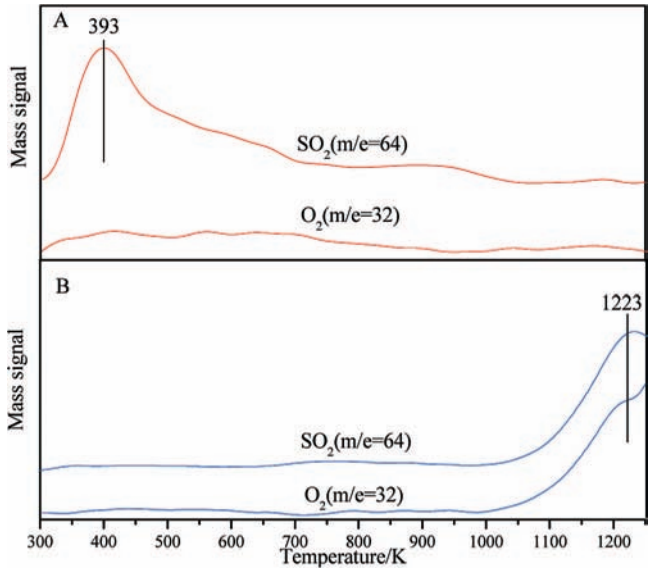

Figure 8. TPD spectra of SO_2 (m/e = 64) and O_2 (m/e = 32) of γ-Al_2O_3 reacted with 200 ppm SO_2 + O_2 (20%) + N_2 for 12 h at 303 K in the absence of NO (A) and in the presence of NO (B).

stages of the reaction. Although the relative intensities of the nitrate features in Figure 7 are different from that in Figure 1, the coordination types of surface species on γ-Al_2O_3 are almost the same. In the presence of water, the relative intensity of the water-solvated nitrate features (1425 and 1320 cm^{-1}) was stronger than that without water. It is suggested that the preadsorbed water only change the ratio between oxide-coordinated and water-solvated surface nitrate,[15] but not promote the formation of N_2O_4 on γ-Al_2O_3 surface. Therefore, we can ascertain that the formation of N_2O_4 is related to the active sites for the adsorbed NO_2 to form nitrite occupied by S (IV) species on alumina.

TPD Experiments. To further identify the surface sulfur species formed on SO_2 saturated γ-Al_2O_3, we also examined TPD curves for γ-Al_2O_3 after exposure to 200 ppm SO_2 balanced with synthesized air in the absence and presence of NO (200 ppm). As shown in Figure 8A, the main peak at 393 K was due to desorption of weakly adsorbed S(IV) when γ-Al_2O_3 sample was exposed to SO_2 without NO. No O_2 signal was observed when NO was absent. In contrast, a peak at 1223 K was observed on the SO_2 reacted sample in the presence of NO (Figure 8B), which could be attributed to the decomposition of aluminum sulfate.[34] The formation of sulfate was also confirmed by the accompanying desorption of O_2. It is evident that at room temperature, SO_2 can only adsorb on alumina surface to form S(IV) under air condition and can be oxidized to sulfate in the presence of NO. These results are in good agreement with the DRIFTS results (Figure 3 and Figure 5).

Discussion

The synergic effect between SO_2 and NO_2 on alumina surface contains two aspects. For NO_2, the reaction pathway was altered. Nitrite as an intermediate was replaced by N_2O_4 in the presence of SO_2. N_2O_4 was observed on hydrated silicon dioxide surface[14] and on porous glass surface in the presence of surface water.[13] Finlayson−Pitts and co-worker[31] explained the accumulation of N_2O_4 on the surface in the presence of water by the results that the Henry's law coefficient for N_2O_4 in water is approximately 2 orders of magnitude larger than that for NO_2. However, this interpretation is not suitable in this work because N_2O_4 was observed only when SO_2 was present (Figure 2) but not on the water preadsorbed alumina surface without SO_2 (Figure 7). It seems that there is a competitive adsorption between NO_2 and SO_2 on the γ-Al_2O_3 surface and the alumina surface is more reactive to SO_2 than to NO_2. As a result, the sites for the formation of nitrite were occupied by SO_2 and N_2O_4 was observed. The assumed different reactivity of alumina to SO_2 and NO_2 was in agreement with the true uptake coefficients of SO_2 and NO_2 on alumina reported by Grassian and co-workers.[11,21] The mechanism of NO_2 adsorption on oxides surface postulated by Underwood et al.[11] suggested that NO_2 adsorbed on surface directly to form nitrite followed by oxidation to nitrate. In fact, the bands of both nitrite and nitrate species were observed in the early spectra (Figure 2) which implied nitrite and nitrate species were yielded synchronously. Therefore, in the presence of SO_2, we postulate that NO_2 first dimerize to N_2O_4 on the surface, followed by the disproportion reaction involving surface oxygen to nitrite and nitrate species, or by the redox reaction with surface tetravalent sulfur species. The reaction steps might be as follows:

$$2NO_2 \leftrightarrows N_2O_4 \quad (1)$$

$$N_2O_4 + M - O \rightarrow MNO_2 + MNO_3 \quad (2)$$

$$N_2O_4 + S(IV) \rightarrow MNO_2 + S(VI) \quad (3)$$

$$MNO_2 + NO + O_2 \rightarrow MNO_3 \quad (4)$$

where M represents surface metal sites, S(IV) and S(VI) represent surface tetravalent and hexavalent sulfur species, respectively.

On the other hand, the synergic effect provides a new formation pathway of sulfate. It is well-known that sulfate aerosols can affect climate directly and indirectly.[16] However, the formation mechanism of secondary sulfate in troposphere is not clear yet. It seems that SO_2 can hardly be oxidized to sulfate on alumina surface at room temperature under air condition.[20–22,38,39] Ullerstam et al.[22] concluded that SO_2 could adsorb on mineral aerosols surface to form sulfite and bisulfite, but an oxidant is needed for the formation of sulfate. Ozone and hydroxyl radical are two familiar oxidants for the formation of sulfate. NO_2 is also considered as an oxidant for the oxidation of SO_2 on mineral oxide surface.[29] It is possible that NO_2 plays a more efficient oxidizer for heterogeneous reactions than O_2.[40] In this work, N_2O_4, the dimer of NO_2, was observed as the oxidant for the formation of sulfate. N_2O_4 in solution and/or at low temperatures is known to isomerize and autoionize to

$NO^+NO_3^-$.[31,41–43] Reaction of this ionic form with water may then generate HONO + HNO_3. Therefore, N_2O_4 was considered as a key intermediate in the heterogeneous hydrolysis of NO_2 which led to the formation of HONO and HNO_3.[13,14] It is well-known that surface oxygen is very important for many reactions on oxides surface. In this work, no band due to NO^+ (2217 cm^{-1})[31,43] was observed because it might react promptly with surface oxygen (O^{2-}) to form nitrite (NO_2^-) species. This reaction pathway was depicted in reaction 2. In addition, it is true, as two early reviews by Riebsomer[44] and Addison[45] shown, that N_2O_4 can oxidize many organic and inorganic compounds rapidly. Oxidative properties of N_2O_4 toward inorganic compounds are selective in that they involve the donation of oxygen atoms rather than the removal of electrons from metal atoms.[45] In this study, we deduce that N_2O_4 was the oxidant of surface sulfite to sulfate. The reaction process may involve surface oxygen as follows:

$$M - N_2O_4 + M - SO_3 \rightarrow M - NONO_2 + M - SO_4 \quad (5)$$

$$M - NONO_2 + M - O \rightarrow 2M - NO_2 \quad (6)$$

where M represents surface Al sites. Nitrite species could be oxidized to nitrate via eq 4 in the flow system (Figure 2) when gas phase NO_2 was present. As a result, nitrate and sulfate were both found on the surface.

Conclusion and Atmospheric Implication

The synergistic effect between NO_2 and SO_2 on alumina oxide at 303 K was investigated to demonstrate the correlation between nitrate and sulfate on mineral oxides. The heterogeneous reaction pathway for NO_2 to nitrates was changed in the presence of SO_2 compared to NO_2 adsorption solely, namely, nitrite as an intermediate was replaced by N_2O_4. On the other hand, SO_2 could be oxidized to sulfate in the presence of NO_2, while only tetravalent sulfur species were formed on alumina without NO_2 in the feed gases.

As mentioned in the Introduction, SO_2 and NOx coexist in the troposphere at ppbv levels. The synergistic interaction between SO_2 and NO_2 on mineral dust should take place widely. This synergistic process not only alters the reaction pathway of NO_2 to nitrate but also provides a new pathway for the formation of secondary sulfate aerosols in the troposphere. Our results also implied that this synergistic heterogeneous reaction is the inherent reason for an internal mixture of nitrate and sulfate in mineral dusts or particles originating from soil.

Acknowledgment. This research was funded by the Ministry of Science and Technology, China (2007CB407301) and National Natural Science Foundation of China (20425722, 50621804).

References and Notes

(1) Song, C. H.; Carmichael, G. R. *Atmos. Environ.* **1999**, *33*, 2203–2218.
(2) Sillman, S.; Logan, J. A.; Wofsy, S. C. *J. Geophys. Res.* **1990**, *95*, 1837–1851.
(3) Beichert, P.; Finlayson-Pitts, B. J. *J. Phys. Chem.* **1996**, *100*, 15218.
(4) Vogt, R.; Finlayson-Pitts, B. J. *J. Phys. Chem.* **1994**, *98*, 3747.
(5) Peters, S. J.; Ewing, G. E. *J. Phys. Chem.* **1996**, *100*, 14093.
(6) Leu, M. T.; Timonen, R. S.; Keyser, L. F.; Yung, Y. L. *J. Phys. Chem.* **1995**, *99*, 13203.
(7) Tabor, K.; Gutzwiller, L.; Rossi, M. J. *J. Phys. Chem.* **1994**, *98*, 6172.
(8) Kalberer, M.; Tabor, K.; Ammann, M.; Parrat, Y.; Weingartner, E.; Piguet, D.; Jost, D. T.; Turler, A.; Gaggeler, H. W.; Baltensperger, U. *J. Phys. Chem.* **1996**, *100*, 15487.
(9) Kirchner, U.; Scheer, V.; Vogt, R. *J. Phys. Chem. A* **2000**, *104*, 8908–8915.
(10) Amman, M.; Kalberer, M.; Jost, D. T.; Tobler, L.; Rossler, E.; Piguet, D.; Gaggeler, H. W.; Baltensperger, U. *Nature* **1998**, *395*, 157.
(11) Underwood, G. M.; Miller, T. M.; Grassian, V. H. *J. Phys. Chem. A* **1999**, *103*, 6184–6190.
(12) Börensen, C.; Kirchner, U.; Scheer, V.; Vogt, R.; Zellner, R. *J. Phys. Chem. A* **2000**, *104*, 5036–5045.
(13) Barney, W. S.; Finlayson-Pitts, B. J. *J. Phys. Chem. A* **2000**, *104*, 171–175.
(14) Goodman, A. L.; Underwood, G. M.; Grassian, V. H. *J. Phys. Chem. A* **1999**, *103*, 7217–7223.
(15) Miller, T. M.; Grassian, V. H. *Geophys. Res. Lett.* **1998**, *25*, 3835–3838.
(16) Dentener, F. J.; Carmichael, G. R.; Zhang, Y.; Leieveld, J.; Crutzen, P. J. *J. Geophys. Res.* **1996**, *101*, 22869–889.
(17) Jayne, J. T.; Davidovits, P.; Worsnop, D. R.; Zahniser, M. S.; Kolb, C. E. *J. Phys. Chem.* **1990**, *94*, 6041–6048.
(18) Sieving, H.; Boatman, J.; Gorman, E.; Kim, Y.; Anderson, L.; Ennis, G.; Luria, M.; Pandis, S. *Nature.* **1991**, *360*, 571–573.
(19) Capaldo, K.; Corbett, J. J.; Kasibhatla, P.; Fischbeck, P.; Pandis, S. N. *Nature* **1999**, *400*, 743–746.
(20) Li, L.; Chen, M.; Zhang, Y. H.; Zhu, T.; Ding, J. *Atmos. Chem. Phys.* **2006**, *6*, 2453–2464.
(21) Goodman, A. L.; Li, P.; Usher, C. R.; Grassian, V. H. *J. Phys. Chem. A* **2001**, *105*, 6109–6120.
(22) Ullerstam, M.; Vogt, R.; Langerb, S.; Ljungström, E. *Phys. Chem. Chem. Phys.* **2002**, *4*, 4694–4699.
(23) Laskin, A.; Gaspar, D. J.; Wang, W. H.; Hunt, S. W.; Cowin, J. P.; Colson, S. D.; Finlayson-Pitts, B. J. *Science* **2003**, *301*, 340–344.
(24) D'Almeida, G. A.; Guillaume, A. *J. Geophys. Res.* **1987**, *92*, 3017–3026.
(25) Tegen, I.; Fung, I. *J. Geophys. Res.* **1994**, *D11*, 22–897, 914.
(26) Zhang, Y.; Carmichael, G. R. *J. App. Meteo.* **1999**, *38*, 353–366.
(27) Ravishankara, A. R. *Science* **2007**, *276*, 1058–1065.
(28) Zhang, D. Z.; Shi, G. Y.; Hu, M. *Atmos. Environ.* **2000**, *34*, 2669–2679.
(29) Ullerstam, M.; Johnson, M. S.; Vogt, R.; Ljungström, E. *Atmos. Chem. Phys.* **2003**, *3*, 2043–2051.
(30) Goodman, A. L.; Bernard, E. T.; Grassian, V. H. *J. Phys. Chem. A* **2001**, *105*, 6443–6457.
(31) Finlayson-Pitts, B. J.; Wingen, L. M.; Sumner, A. L.; Syomin, D.; Ramazan, K. A. *Phys. Chem. Chem. Phys.* **2003**, *5*, 223–242.
(32) Wang, J.; Koel, B. E. *J. Phys. Chem. A* **1998**, *102*, 8573–8579.
(33) Bazin, P.; Saur, O.; Lavalley, J. C.; Blanchard, G.; Visciglio, V.; Touret, O. *Appl. Catal., B* **1997**, *13*, 265–274.
(34) Wu, Q.; Gao, H. W.; He, H. *J. Phys. Chem. B* **2006**, *110*, 8320–8324.
(35) Liu, J. F.; Yu, Y. B.; Mu, Y. J.; He, H. *J. Phys. Chem. B* **2006**, *110*, 3225–3230.
(36) Goodman, A. L.; Bernard, E. T.; Grassian, V. H. *J. Phys. Chem. A* **2001**, *105*, 6443–6457.
(37) Peri, J. B.; Hannan, R. B. *J. Phys. Chem.* **1960**, *65*, 1526–1530.
(38) Karge, H. G.; Dalla-Lana, I. G. *J. Phys. Chem.* **1984**, *88*, 1538–1543.
(39) Datta, A.; Cavell, R. G.; Tower, R. W.; George, Z. M. *J. Phys. Chem.* **1985**, *89*, 443–449.
(40) Koebel, M.; Madia, G.; Raimondi, F.; Wokaun, A. *J. Cata.* **2002**, *209*, 159.
(41) Addison, C. C. *Angew. Chem.* **1960**, *72*, 193.
(42) Goulden, J. D. S.; Millen, D. J. *J. Chem. Soc.* **1950**, 2620.
(43) Hellebust, S.; Roddis, T.; Sodeau, J. R. *J. Phys. Chem. A* **2007**, *111*, 1167–1171.
(44) Riebsomer, J. L. *Chem. Rev.* **1945**, *36*, 157.
(45) Addison, C. C. *Chem. Rev.* **1980**, *80*, 21–39.

JP802025Z